

Beneficial effects of Co^{2+} on co-electrodeposited Ni-SiC nanocomposite coating

YANG Xiu-ying(杨秀英)^{1,2}, LI Kang-ju(李康举)¹, PENG Xiao(彭晓)², WANG Fu-hui(王福会)²

1. Polytechnic School, Shenyang Ligong University, Fushun 113122, China;
2. State Key Laboratory for Corrosion and Protection, Institute of Metal Research, Chinese Academy of Sciences, Shenyang 110016, China

Received 22 February 2008; accepted 13 June 2008

Abstract: Ni-SiC nanocomposites were fabricated by co-electrodeposition of nickel with silicon carbide nanoparticles on the pure nickel substrates from a nickel sulfate bath with and without the addition of Co^{2+} . The presence of Co^{2+} in the electrolyte modifies the Ni matrix to Ni-Co solid solution matrix. It helps to refine the grain size of the nanocomposite coating and improves the content of SiC dispersed in the matrix, and consequently results in higher microhardness. The cathodic polarization curves and electrochemical impedance spectroscopy (EIS) at cathodic potential were investigated in the electrolyte with and without Co^{2+} . A modified cathodic polarization curve with a positive shift in reduction potential and a smaller capacitive loop of EIS are observed. These are attributed to the strong adsorption of Co^{2+} on the SiC nanoparticles. Consequently, it increases the forces of electrostatic attraction between the SiC nanoparticles and the cathode, which promotes the codeposition of SiC nanoparticles in the matrix.

Key words: Ni-SiC; Co^{2+} addition; co-electrodeposition; nanocomposite

1 Introduction

Composite electrodeposition is a cost-effective method suitable for producing metal matrix composites coatings consisting of a metal or alloy matrix and dispersed second phase particles[1]. The second particles can be hard oxides and carbide particles like Al_2O_3 , Cr_3C_2 , SiC or diamond, solid lubricants like PTFE or graphite for improving the wear, corrosion resistance and/or reducing the friction coefficient[2–9]. Ni-SiC coatings are largely introduced in car engine manufacturing or combustion engines and have already demonstrated their efficiency as anti-wear coatings [10–12]. The properties of these coatings depend mainly on the content of the particles codeposited in the coatings and on the size of particles[6–8]. Recently, much interest is paid on co-electrodeposited Ni-SiC coatings with fine particle sizes, especially nanoparticles, since they can impart the coating the improved and well-controlled properties[8–10]. However, the percentage nano-sized particles codeposited in the coatings is the limiting factor [5,7].

Many factors influence the codeposition such as the

particle size and metal matrix type, applied current density (or potential), solution hydrodynamics, and solution concentrations. In addition, attempts to increase the co-deposition of particles using various organic surfactants in the deposits have been reported[8–9]. Unfortunately, the addition of organic additives can cause such disadvantages as instability in the electrolyte, high stress or brittleness of the composite deposits. Thus, there is a strong motivation for the development of alternative additives that can improve the incorporation rate of the particles in the metal matrix.

The aim of the present work is to study the effects of inorganic additives Co^{2+} on the codeposition of SiC nanoparticle as well as the Ni matrix of the deposits by characterizing the microstructure using SEM/EDS and XRD. To understand the influence of Co^{2+} on the co-electrodeposition of Ni-SiC, the cathodic polarization curves and electrochemical impedance spectroscopy (EIS) were also investigated.

2 Experimental

The nickel and β -SiC nanoparticles were co-electrodeposited onto the pure nickel substrates from

nickel sulfate bath without and with the addition of Co^{2+} (0.05 mol/L). The bath compositions and electro-deposition parameters are listed in Table 1. Prior to the codeposition, the SiC particles were ultrasonically dispersed in the bath for 30 min. During coating preparation, a reciprocating perforated plate was used to maintain the nanoparticles suspending in the bath as described previously[13–14]. TEM bright-field image showed that the silicon carbide nanoparticles are in spherical or spherical-like shapes and have an average size of 45 nm, as indicated in Fig.1. The as-deposited composite coatings were characterized by SEM/EDS and XRD.

Table 1 Compositions and parameters of nickel sulfate bath for nanocomposite coatings

$\rho(\text{NiSO}_4 \cdot 6\text{H}_2\text{O})/(\text{g} \cdot \text{L}^{-1})$	$\rho(\text{H}_3\text{BO}_3)/(\text{g} \cdot \text{L}^{-1})$	$\rho(\text{NH}_4\text{Cl})/(\text{g} \cdot \text{L}^{-1})$	
150	15	15	
$\rho(\text{SiC})/(\text{g} \cdot \text{L}^{-1})$	Current density/ $(\text{A} \cdot \text{dm}^{-2})$	Temperature/ $^{\circ}\text{C}$	pH
20	3	30	4.5–5.4

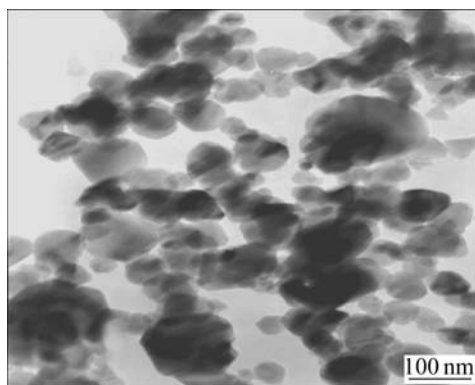


Fig.1 TEM image of β -SiC particles

The microhardness was measured with SHIMADZU Vickers hardness tester under a load of 2 N for 10 s. The final value quoted for the micro-hardness of a deposit was the average of 5 measurements.

Electrochemical investigations were performed using an EG&G PAR 273 electrochemical apparatus. Standard three-electrode system was used in the electrochemical test with a saturated calomel electrode (SCE) as the reference electrode, a platinum sheet as the auxiliary electrode (AE), and the sample as the working electrode (WE). Magnetic stirring was employed at the cell bottom to maintain a uniform particle concentration in the bulk solution. The potentiodynamic polarization at a constant scan rate of 0.5 mV/s was conducted from -0.2 to 1.6 V. Electrochemical impedance spectra were acquired in the frequency range of 10^{-2} – 10^5 Hz with a 0.5 mV amplitude sine wave generated by a frequency

response analyzer.

3 Results and discussion

3.1 Influence of Co^{2+} on deposited nickel matrix

Fig.2 shows the effect of Co^{2+} concentration on the composition of the matrix at a fixed concentration of Ni^{2+} ion in the sulfate electrolytes. It is clearly observed that the Co content in the matrix increases gradually with Co^{2+} concentration in the bath. Meanwhile, the percentage of Co in the matrix is always higher than that in the solution. This has been confirmed by the anomalous codeposition of Ni-Co solid solution alloy. Namely, the less noble metal (Co) is preferentially deposited. These phenomena are attributed to the changes of the near electrode pH, the formation of metal hydroxyl and competitive adsorption[15–16].

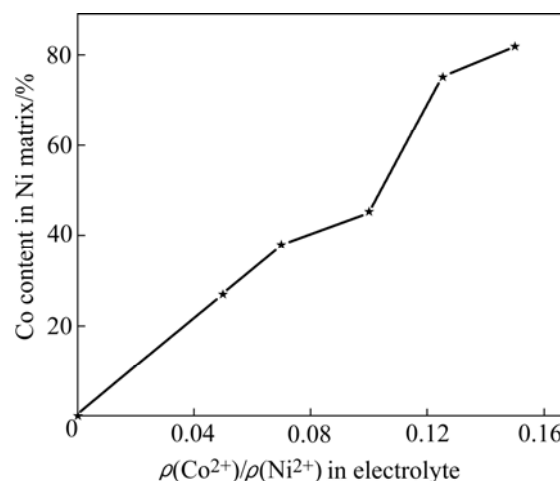


Fig.2 Effect of Co^{2+} concentration on composition of Ni matrix

Fig.3 shows typical surface morphologies of Ni/Ni-Co alloys with different Co content. Fig.3(a) presents a typical morphology of Ni deposit with relatively large grain size. Sequentially increasing Co content from 27% to 45% (Figs.3(b)–(c)) results in a gradual decrease in the grain size. However, when increasing Co content up to 82% (Fig.3(d)), the morphology of the Ni-Co alloy changes dramatically, leading to a regular branched structure.

Fig.4 gives the microhardness of Ni-Co alloys as a function of Co content. The maximum hardness appears at approximately 45% Co (0.05 mol/L Co^{2+} in the bath), which is associated with the microstructural modification.

3.2 Characterization of Ni-SiC nanocomposite with and without addition of Co^{2+}

From the results mentioned above, 0.05 mol/L Co^{2+} in the bath exerts great influence on the deposited Ni matrix including microstructure and microhardness.

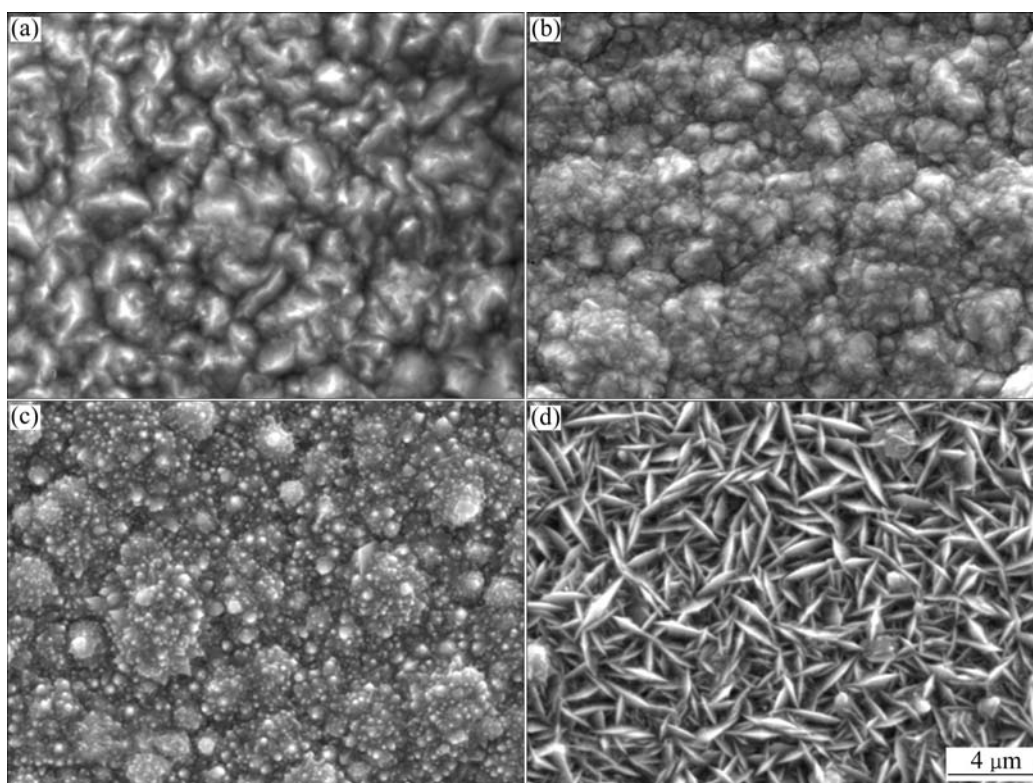


Fig.3 Surface morphologies of as-deposited Ni (a), Ni-27%Co (b), Ni-45%Co (c) and Ni-82%Co (d)

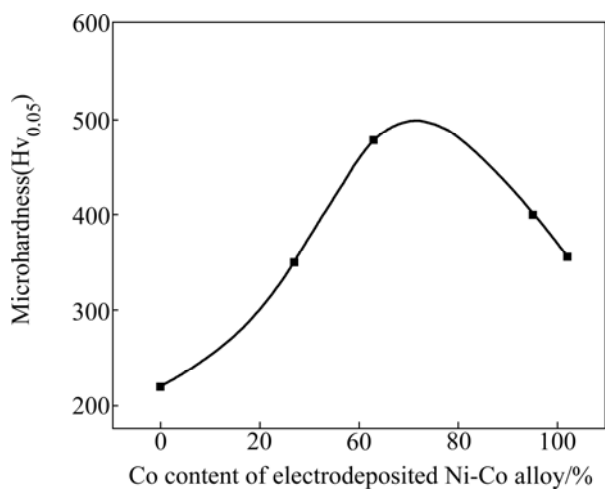


Fig.4 Microhardness of Ni-Co deposit as function of Co content

Hence, on the effect of 0.05 mol/L Co^{2+} on the co-electrodeposited Ni-SiC nanocomposite is focused on. Fig.5 shows the low-magnification and high-magnification surface morphologies of Ni-SiC with and without Co^{2+} addition. EDAX analysis indicates that the content of Si in the nanocomposite increases from 3.1% without Co^{2+} addition to 6.6% with Co^{2+} addition. From Fig.5, firstly it can be seen that Ni-SiC nanocomposites with the presence of Co^{2+} have a smoother surface than the Co-free one (Figs.5(a) and (b)). Secondly, the grain refinement is observed as shown in Fig.5(c) and Fig.5(d).

The FWHM of the Bragg line for the (111) and (220) peaks of XRD patterns from the Ni matrix with Co^{2+} addition is broadened in comparison with that from Co-free one as shown in Fig.6. This also illustrates that the addition of Co^{2+} refines the grains of the matrix. Meanwhile, peaks of Si in the nanocomposite become strong with the addition of Co^{2+} . This agrees well with the EDAX results. GUGLIELMI[17] proposed a successive two-step adsorption mechanism for the incorporation of inert particles during the codeposition process. They are loose adsorption and strong adsorption. The second step is thought to be the rate controlled step in the codeposition of particles, which is assumed to be electric field assisted. According to the previous reports[3,18], Co^{2+} are adsorbed on nano-SiC particles much easier compared with Ni^{2+} . This might give particle surfaces a more positive charge, which means that the forces of electrostatic attraction between the nano-SiC particles and the negatively charged cathode will be increased. As a result, a higher content of nano-SiC particles is codeposited in the matrix with the Co^{2+} addition. Furthermore, the electrodeposition process is a competition between nucleation and crystal growth. The included nano-SiC particles can act as nucleation sites and therefore as a detriment to crystal growth. Hence, the crystal growth is inhibited and the grains are refined, which is in good agreement with the experimental results.

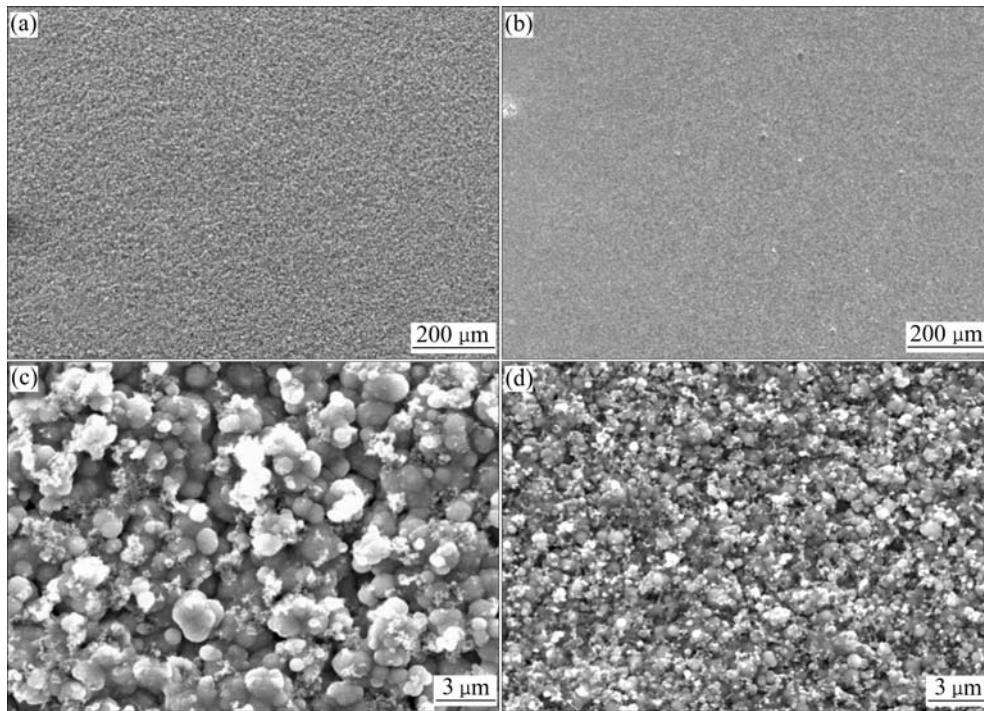


Fig.5 Surface morphologies of as-deposited Ni-SiC (a, c) and (Ni-Co)-SiC nanocomposites (b, d): (c) Magnified morphology of (a); (d) Magnified morphology of (a)

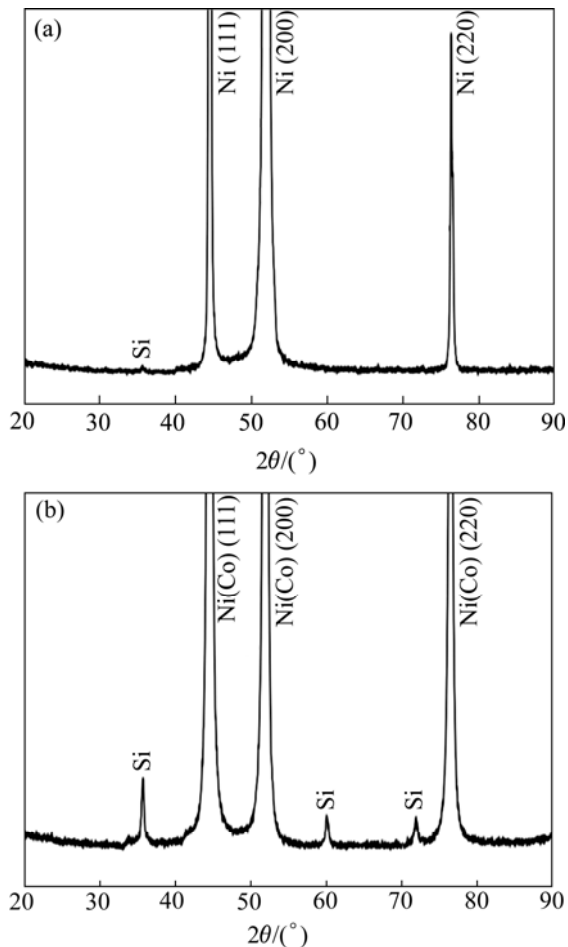


Fig.6 XRD patterns of as-deposited Ni-SiC (a) and Ni-45Co-SiC nanocomposites (b)

3.3 Microhardness of Ni-SiC with and without addition of Co^{2+}

Fig.7 gives the microhardness of Ni-SiC nanocomposites with and without the addition of Co^{2+} . Clearly, the Ni-SiC nanocomposite exhibits higher microhardness with adding 0.05 mol/L Co^{2+} . It is well known that the hardness of metal matrix composites depends on the amount of the dispersed phase and the matrix[11]. First, Ni-Co solid solution matrix has the higher hardness than the Ni matrix[12]. Second, the dispersed hard phase SiC increases with Co addition, consequently higher hardness can be observed. Third, the grain refinement brought by 0.05 mol/L Co^{2+} also contributes to the higher microhardness.

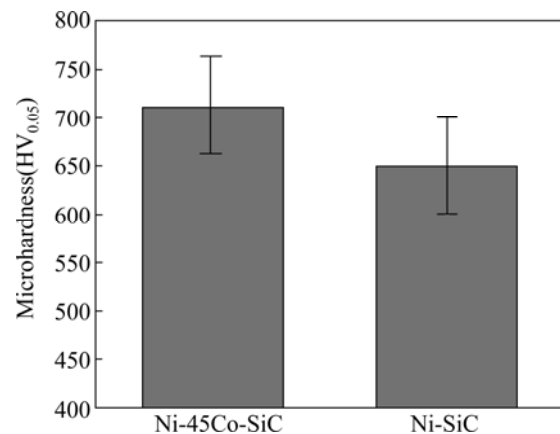


Fig.7 Microhardness of Ni-SiC and Ni-45Co-SiC

3.4 Polarization curves of Ni-SiC nanocomposites with and without addition of Co^{2+}

Fig.8 presents the cathodic potentiodynamic curves for codeposition of Ni-SiC nanocomposite with and without Co^{2+} . Co^{2+} addition leads to a potential shift to more positive direction with the unchanged slopes, demonstrating that the co-deposition of SiC is promoted in the presentation of Co^{2+} . However, the electrochemical reaction mechanism is not affected significantly. It has been reported that the nanoparticles are surrounded by a thin layer of Ni^{2+} and H_3O^+ ions adsorbed after the particles are introduced into the electrolyte[19]. While Co^{2+} is much easier adsorbed on the nanoparticles than Ni^{2+} [3,18]. Therefore, in the case of the present results, the shift in reduction potential is attributed to the increasing Co^{2+} on the surfaces of the SiC nanoparticles, which can decrease the cathodic polarization and promote the electrodeposition process.

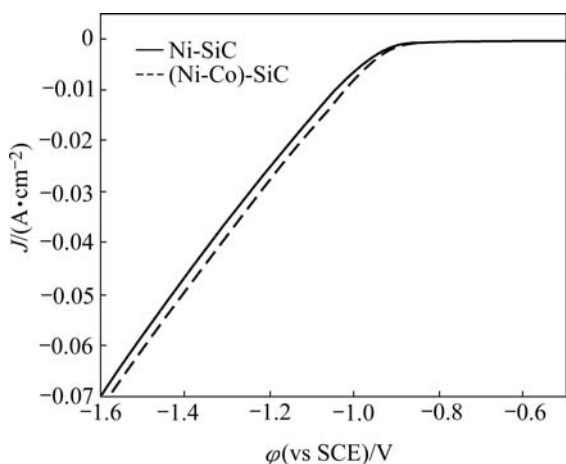


Fig.8 Cathodic potentiodynamic curves for codeposition of Ni-SiC nanocomposite with and without Co^{2+} addition

3.5 EIS of Ni-SiC with and without addition of Co^{2+}

To further distinguish the effects of inorganic additives Co^{2+} on the deposition of Ni-SiC, electrochemical impedance spectroscopy (EIS) was conducted. Fig.9 shows the EIS (Nyquist plots) of Ni-SiC nanocomposite with and without Co^{2+} addition. Clearly, co-electrodeposition of Ni-SiC with and without Co^{2+} addition is a multi-step reaction process including surface adsorbing intermediates produced by the charge transfer reaction and the removal of the adsorbed intermediates by a subsequent consumption reaction. At high frequency, with the addition of Co^{2+} , one smaller capacitive loop is obtained besides one similar inductive loop at low frequency. The capacitive loop can be interpreted as the electrical double layer capacitance C_{dl} parallel to a charge transfer resistance R_{ct} . The inductive loop may result from the adsorption/desorption of intermediates in the electrolyte and electrode interface[20].

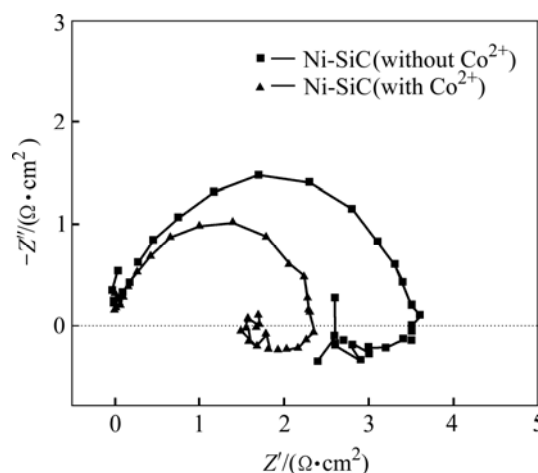


Fig.9 EIS of Ni-SiC nanocomposite with and without Co^{2+} addition

Fig.10 shows the equivalent circuit representing the electrochemical behaviour of codeposition of SiC nanoparticles with Ni-Co solid solution matrix. In this circuit, R_{el} represents the electrolyte resistance, R_{ct} the charge transfer resistance, C_{dl} the double layer capacitance, L_1 the inductance and R_1 the resistance from the adsorbed/desorbed intermediates or other species on the electrode surface. The magnitude of R_{ct} is an indicator of the easiness of the electrochemical reaction. According to the equivalent circuit, the fitting results of the impedance parameters for the codeposition of the Ni-SiC show that the addition of Co^{2+} leads to the decrease of R_{ct} from $3.57 \Omega \cdot \text{cm}^2$ to $2.34 \Omega \cdot \text{cm}^2$, suggesting that Co^{2+} activates the codeposition of Ni-SiC, which is in good agreement with the results of polarization curves.

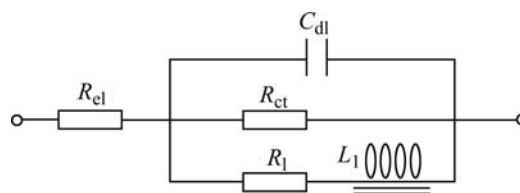


Fig.10 Equivalent circuit used for simulating impedance spectra for codeposition of Ni-SiC with Co^{2+}

4 Conclusions

1) The effects of inorganic additives Co^{2+} on the codeposition of SiC nanoparticle as well as on the Ni matrix of the deposits were investigated. The presence of the Co^{2+} in the electrolyte modifies the Ni matrix to Ni-Co solid solution matrix, refines the grain size of the nanocomposite coating, improves the content of the SiC dispersed in the matrix and results in the higher micro-hardness.

2) Investigations on the cathodic polarization curves

and the electrochemical impedance spectroscopy(EIS) show that a modified cathodic polarization curve with a positive shift in reduction potential and a smaller capacitive loop in the EIS are attributed to the strong adsorption of Co^{2+} on the SiC nanoparticles. Consequently, the forces of electrostatic attraction between the SiC nanoparticles and the cathode are increased. Therefore, the codeposition of SiC nanoparticles in the matrix is promoted.

References

- [1] WANG B Q, LUER K. The erosion-oxidation behavior of HVOF Cr_3C_2 -NiCr cermet coating [J]. *Wear*, 1994, 174: 177–185.
- [2] HOVESTAD A, JANSEN L J J. Electrochemical codeposition of inert particles in a metallic matrix [J]. *J Appl Electrochem*, 1995, 25: 519–527.
- [3] WU G, LI N, ZHOU D, MITSUO K. Electrodeposited Co-Ni- Al_2O_3 composite coatings [J]. *Surf Coat Technol*, 2004, 176: 157–164.
- [4] KERR C, BARKER D, WALSH F, ARCHER J. The electrodeposition of composite coatings based on metal matrix-included particle deposits [J]. *Trans IMF*, 2000, 78: 171–178.
- [5] YANG Zhi, XU Hui, LI Meng-ke, SHI Yan-li, HUANG Yi, LI Hu-lin. Preparation and properties of Ni/P/single-walled carbon nanotubes composite coatings by means of electroless plating [J]. *Thin Solid Films*, 2004, 466: 86–91.
- [6] SERHA Z, MORVAN J, BERC P, REZRAZE M, PAGETTI J. Determination of the incorporation rate of PTFE particles in Au-Co-PTFE composite coatings by infrared reflection absorption spectroscopy [J]. *Surf Coat Technol*, 2001, 145: 233–241.
- [7] NARAYAN R, NARAYANA B H. Electrodeposited chromium-graphite composite coatings [J]. *J Electrochem Soc*, 1981, 128(8): 1704–1708.
- [8] HUANG Y S, ZENG X T, HU X F, LIU F M. Corrosion resistance properties of electroless nickel composite coatings [J]. *Electrochem Acta*, 2004, 49: 4313–4319.
- [9] GYFTOU P, STROUMBOULI M, PAVLATOU E A, ASIMIDIS P, SPYRELLIS N. Tribological study of Ni matrix composite coatings containing nano and micro SiC particles [J]. *Electrochim Acta*, 2005, 50: 4544–4550.
- [10] BENE L, BONORA P L, BORLLO A, MARTELLI S, WENGER F, PONTIAUX P, GALLAND J. Composite electrodeposition to obtain nanostructured coatings [J]. *J Electrochem Soc*, 2001, 148: C461–C465.
- [11] GARCIA I, FRANSAER J, CELIS J P. Improved corrosion resistance through microstructural modifications induced by codepositing SiC-particles with electrolytic nickel [J]. *Corros Sci*, 2003, 45: 1173–1189.
- [12] HOVESTAD A, JANSSEN L J J. Electrochemical codeposition of inert particles in a metallic matrix [J]. *Appl Electrochem*, 1995, 25: 519–527.
- [13] PENG X, PING D, LI T, WU W. Oxidation behavior of a Ni- La_2O_3 codeposited film on nickel [J]. *J Electrochem Soc*, 1998, 145: 389–398.
- [14] PENG X, PING D, LI T, WU W. Effect of La_2O_3 particles on the oxidation of electro-deposited nickel films [J]. *Oxid Met*, 1999, 51: 291–315.
- [15] ZECH N, POKLAHA E J, LANDOLT D. Anomalous codeposition of iron group metals (I): Experimental results [J]. *J Electrochem Soc*, 1999, 146: 2886–2891.
- [16] GOLODNITSKY D, GUDIN N V, VOLYANUK G A. Study of nickel-cobalt alloy electrodeposition from a sulfamate electrolyte with different anion additives [J]. *J Electrochem Soc*, 2000, 147: 4156–4163.
- [17] GUGLIELMI N. Kinetics of the deposition of inert particles from electrolytic baths [J]. *J Electrochem Soc*, 1972, 119: 1009–1012.
- [18] WU G, LI N, ZHOU D, MITSUO KURACHI. Effect of Al_2O_3 particles on the electrochemical codeposition of Co-Ni alloys from sulfamate electrolytes [J]. *Mater Chem Phys*, 2004, 87: 411–419.
- [19] BENE L, BONORA P L, BORLLO A. Preparation and investigation of nanostructured SiC-nickel layers by electrodeposition [J]. *Solid State Ionics*, 2002, 151: 89–95.
- [20] YE H S H, WAN C C. Codeposition of SiC powders with nickel in a Watts bath [J]. *J Appl Electrochem*, 1994, 24: 993–1000.

(Edited by YANG Bing)